

Computer-based simulation of kinetics of internal corrosion of engineering alloys at high-temperatures

(Simulação computacional da cinética de corrosão interna de ligas metálicas usadas em altas temperaturas)

Vicente Braz Trindade

Institute for Materials Science - University of Siegen / Germany. E-mail: vicentebraz@yahoo.com.br

Hans-Jürgen Christ

Institute for Materials Science - University of Siegen / Germany. E-mail: crist@ifwt.mb.uni-siegen.de

Ulrich Krupp

Applied University of Osnabrück / Germany. E-mail: u-krupp@fh-osnabrueck.de

Resumo

Uma previsão razoável da durabilidade de estruturas ou equipamentos que operam em temperaturas elevadas e atmosferas agressivas requer um completo entendimento dos mecanismos de degradação dos materiais causados por cargas mecânicas e corrosão. O objetivo geral desse estudo é simular processos de corrosão em temperaturas elevadas em condições próximas àquelas encontradas na realidade. Isto requer um modelo termodinâmico para prever a estabilidade das fases e um modelamento matemático que descreva os processos cinéticos, por exemplo, difusão no estado sólido - difusão no interior do grão e ao longo dos contornos de grão. Um programa computacional foi desenvolvido para descrever a oxidação interna, nitretação e sulfetação de várias ligas comerciais. O subprograma termodinâmico ChemApp foi integrado em um modelo numérico que usa o método de diferenças finitas. O modelo desenvolvido simula processos de corrosão interna que são controlados por difusão no estado sólido e que envolvam precipitação de várias fases. Formação de zona de corrosão interna, incluindo corrosão intercrystalina em aços contendo baixo teor de Cr, é também tratada pelo modelo computacional desenvolvido. Nesse artigo, são consideradas soluções diluídas e monofásicas.

Palavras-chave: Nitretação interna, oxidação, termodinâmica computacional, ChemApp, InCorr, diferenças finitas.

Abstract

A reasonable prediction of the service life of structures or equipment operating at high-temperatures in aggressive atmospheres requires a full understanding of the degradation mechanisms of the material due to mechanical loading and corrosion. The overall objective of this study is to simulate high-temperature corrosion processes under near-service conditions, which require both, a thermodynamic model to predict phase stabilities for given conditions and a mathematical description of the kinetic process, i.e., solid state diffusion. A computer program was developed in which the thermodynamic program library ChemApp is integrated into a numerical finite-difference diffusion calculation to treat internal oxidation, nitridation and sulfidization processes in various commercial alloys. The model is capable of simulating multi-phase internal corrosion processes controlled by solid-state diffusion into the bulk metal as well as intergranular corrosion occurring in low-alloy steels by fast inward oxygen transport along the grain boundaries of the substrate. In this article, dilute and monophase solutions are considered.

Keywords: Internal nitridation, oxidation, computational thermodynamics, ChemApp, InCorr, finite difference.

1. Introduction

For alloys used in high temperature corrosive atmospheres, the capacity for the formation of a protective scale with high density, high stability, good adhesion and low growth rate on the surface of the component is very important. Generally, Al_2O_3 , SiO_2 and Cr_2O_3 are expected to protect materials against serious high temperature degradation. For most materials the formation of a continuous protective scale is difficult due to the limitation of the maximum content of protective oxide forming elements. If no protective scales are formed on the surface, or if cracks or other types of defects allow rapid transport of corrosive species like oxygen and nitrogen through the scale, internal corrosion becomes possible, which decreases the lifetime of components substantially. A computer-based model that has been developed during the last ten years at the University of Siegen (Krupp, 1998) provides a very useful tool to simulate such degradation processes under complex conditions and, hence, to contribute to new mechanism-based life-prediction methods.

2. Theory of internal corrosion

When the oxygen partial pressure on the surface of the alloy is high enough, particles of oxides or other corrosion products of the less noble element can be formed on the sub-surface of the alloy. This phenomenon is known as internal corrosion. Wagner (1959) developed a theory for the case of internal oxidation, which permits the estimation of the critical concentration of the element B, c_B^{crit} , in the alloy for which there is the transition from the formation of external scale to the formation of internal oxidation zone (oxide BO_x).

$$c_B^{crit} > \left[\frac{\pi g^* c_O D_O V_{Leg}}{2 \nu D_B V_{Ox}} \right]^{1/2} \quad (1)$$

this means:

$c_B > c_B^{crit}$: there is formation of external oxide scale.

$c_B \leq c_B^{crit}$: there is formation of internal oxidation zone.

where:

c_B^{crit} represents the critical concentration of the less noble element B in the alloy.

c_O is the oxygen solubility in the alloy A.

D_O and D_B represent the diffusion coefficient of oxygen and the element B in the alloy, respectively

V_{Leg} and V_{Ox} represent the molar volume of the alloy and the oxide, respectively $g^* = f(V_{Ox} / V_{Leg})$ is a function which describes the relationship between the molar volume of the oxide and the alloy.

Through Eq. (1) it can be noted that critical concentration c_B^{crit} increases by the decreasing on the flux of the element B in the alloy (low c_O) or by increasing the oxygen solubility in the alloy (high c_O).

As the diffusion process is the predominant factor on the kinetics of internal corrosion, the depth of the reaction front can be described by means of a parabolic function

$$\xi = 2\gamma\sqrt{D_O t} \quad (2)$$

where:

D_O is the diffusion coefficient of oxygen in the alloy.

t is the diffusion time.

γ is a dimensionless parameter

The reaction front ξ moves continuously to the interior of the alloy. The internal oxidation rate $D\xi/dt$ is obtained by the derivation of Eq. (2)

$$\frac{d\xi}{dt} = \gamma \left(\frac{D_O}{t} \right)^{1/2} \quad (3)$$

Applying Ficks 2nd law for the case of one dimensional diffusion of oxygen and the alloying element B:

$$\frac{\partial c_O}{\partial t} = D_O \frac{\partial^2 c_O}{\partial x^2} \text{ for } 0 \leq x \leq \xi \quad (4)$$

$$\frac{\partial c_B}{\partial t} = D_B \frac{\partial^2 c_B}{\partial x^2} \text{ for } x \geq \xi \quad (5)$$

If the following initial and boundary conditions are considered:

$$c_O = 0 \text{ for } x \geq \xi \text{ and } t > 0,$$

$$c_O = c_O^s \text{ for } x = 0 \text{ and } t > 0,$$

$$c_B = 0 \text{ for } x \leq \xi \text{ and } t > 0,$$

$$c_B = c_B^0 \text{ for } x \geq 0 \text{ and } t = 0.$$

where:

c_O - is the initial concentration of oxygen soluble in the alloy.

c_B - concentration of the alloying element B.

c_O^s - maximum concentration of oxygen in the alloy (surface concentration).

c_B^0 - initial concentration of the alloying element B.

D_O - diffusion coefficient of oxygen in the alloy.

D_B - diffusion coefficient of the element B in the alloy

The following solutions of Ficks 2nd law" can be derived:

$$c_O(x,t) = c_O^s \left(1 - \frac{\text{erf}\left(\frac{x}{2\sqrt{D_O t}}\right)}{\text{erf}\gamma} \right) \quad (6)$$

$$c_B(x,t) = c_B^0 - \left(1 - \frac{\text{erfc}\left(\frac{x}{2\sqrt{D_B t}}\right)}{\text{erfc}\left(\sqrt{\frac{D_O}{D_B}}\gamma\right)} \right) \quad (7)$$

where erf is the error function and erfc is the complementary error function.

At the reaction front $x = \xi$, the amount of oxygen moving from the alloy surface must be equivalent to the amount

of alloying element B moving to the alloying surface. For the formation of the oxide BO_v at the position ξ , the oxygen flux to the x direction must be v times bigger than the flux of B atoms in the opposite direction. Using Ficks 1st law, the following can be obtained:

$$\lim_{\varepsilon \rightarrow 0} \left[-D_O \left(\frac{\partial c_O}{\partial x} \right)_{x=\xi-\varepsilon} = v D_B \left(\frac{\partial c_B}{\partial x} \right)_{x=\xi+\varepsilon} \right] \quad (8)$$

By replacing Eq. (6) and (7) into Eq. (8):

$$\frac{c_O^s}{c_B^0} = \frac{\text{verf}(\gamma) \exp(\gamma^2)}{\sqrt{\frac{D_O}{D_B}} \text{erfc} \left(\sqrt{\frac{D_O}{D_B}} \gamma \right) \exp \left(\frac{\gamma^2 D_O}{D_B} \right)} \quad (9)$$

From Eq. (9), the parameter γ can be determined. Two limit cases should be considered:

$$(a) \text{ case 1: } \frac{D_B}{D_O} \ll \frac{c_O^s}{c_B^0} \ll 1$$

using Eq. (9) the value of γ is given by:

$$\gamma = \sqrt{\frac{c_O^s}{2v c_B^0}} \quad (10)$$

which gives an oxidation zone depth:

$$\xi = \sqrt{\frac{2c_O^s D_O t}{v c_B^0}} \quad (11)$$

In this case the reaction front movement is determined by the oxygen diffusion coefficient in the alloy and the diffusion of the element B is practically not considered.

$$(b) \text{ case 2: } \frac{c_O^s}{c_B^0} \ll \frac{D_B}{D_O} \ll 1$$

The parameter γ is given by:

$$\gamma = \frac{c_O^s}{2v c_B^0} \sqrt{\frac{\pi D_O}{D_B}} \quad (12)$$

In this case the depth of the internal oxidation zone is calculated according to the following equation:

$$\xi = \frac{c_O^s D_O}{v c_B^0} \sqrt{\frac{\pi}{D_B}} \quad (13)$$

For this condition, the depth of the internal oxidation zone depends also on the diffusion coefficient of the alloying element B.

The theory described above is applied for cases where only one kind of precipitate occurs and this precipitate must be very stable and stoichiometric. This condition is applied only for very limited theoretical cases.

3. Computer simulation of diffusion-controlled corrosion processes

Parameters determining high-temperature corrosion processes include the diffusivities and initial concentrations of all the alloying elements and the diffusivities and initial concentrations of the corrosive species at the interfaces between gas phase and outer scale, outer scale and underlying metal as well as at interfaces between different phases within the scale and within the metal.

Since internal corrosion is mainly governed by the diffusion of the corrosive species, such as O, N, C, or S, and to some extent also of the reacting metallic elements like Ti, Al, or Cr, modelling starts off by solving the diffusion differential equations (Fick's second law) for the respective elements with concentrations C and diffusion coefficients D

$$\frac{dC}{dt} = \nabla(D\nabla C) \quad (14)$$

numerically, using, e.g., the finite-difference technique (Crank, 1975).

The finite-difference solution transfers the gradients of Eq. (14) to difference quotients in a time (T_j)/location (X_j) mesh (here simplified for one-dimensional diffusion problems, see Figure 1a), where the concentrations C_i^{j+1} of the diffusing species at the location step i and the time step $j+1$ are calculated from the two neighbouring concentrations C_{i-1}^{j+1} and C_{i+1}^{j+1} and the concentrations of the preceding time step C_{i-1}^j , C_i^j , and C_{i+1}^j , according to the implicit Crank-Nicholson approach (Crank, 1975):

$$C_i^{j+1} = C_i^j + \frac{D\Delta T}{2\Delta X^2} [(C_{i+1}^{j+1} + C_{i+1}^j) - 2(C_i^{j+1} + C_i^j) + (C_{i-1}^{j+1} + C_{i-1}^j)] \quad (15)$$

Eq. (15) has to be solved simultaneously for all location steps i and can be rewritten in the form

$$-s C_{i-1}^{j+1} + (2+2s) C_i^{j+1} - s C_{i+1}^{j+1} = s C_{i-1}^j + (2-2s) C_i^j + s C_{i+1}^j \quad (16)$$

$$\text{where } s = \frac{D\Delta T}{(\Delta X)^2}.$$

There are three unknown concentrations on the left-hand side of Eq. (16) for the time step $j+1$ and three known values on the right-hand side for the time step j . If there are n grid points along each time row, then for the first time row, $j=0$ and $i=1$, n equations for n unknown concentrations values have to be solved simultaneously, starting with the boundary conditions at the time step $j=0$ (beginning of the diffusion process, all concentrations are set to their initial values) and the location step $i=0$ (known concentration at the interfaces).

Using the finite-difference method, the concentrations of species involved in the oxidation process are calculated in small discrete steps as a function of time and location as described above. Several authors have used the Crank-Nicolson technique to solve the diffusion equation for the description of corrosion processes. Nesbitt (Nesbitt, 1995) and Vedula et al. (Vedula et al, 1981), applied it to internal oxidation, Christ et al. (Christ et al, 1986) to carburisation of Ni-Cr alloys and austenitic steels, Savva et al. (Savva et al, 1996) to nitridation of Ni-Ti alloys, and Krupp and Christ (Krupp, 1998 and Christ, 1986) to internal nitridation of Ni-Cr-Al-Ti alloys.

For a complete description of internal corrosion processes, the diffusion process has to be treated in combination with the thermodynamics of the chemical reaction between the metallic and the corrosive species. For complex systems this can be done by a numerical thermodynamic equilibrium calculation based on the minimization of Gibbs free energy criteria. In the present study, thermodynamic calculations were performed using the commercial software package ChemApp based on specific thermodynamic data sets for the systems under consideration. This software

package was implemented in a numerical FORTRAN diffusion program enabling to simulate diffusion-controlled corrosion processes. Recently, this program termed InCorr has been transferred to the commercial simulation platform MATLAB in order to increase its flexibility, to make it user-friendly (see Figure 1b) and to increase the calculation speed by distributing the thermodynamic equilibrium calculations required for each time-location step in the finite-difference approach to separate processing units (parallel computing by thermodynamic workers, see Figure 1a).

In the framework of the EU project OPTICORR (Trindade et al, 2005) the applicability of InCorr has been extended from pure internal corrosion phenomena, like internal oxidation, carburization and nitridation, to the formation of multi-phase superficial oxide scales, which are formed, e.g. during high-temperature exposure of low-alloy boiler steels (Trindade, 2006). From the various corrosion phenomena that can be treated by InCorr two examples are briefly discussed in the following sections: (i) Internal nitridation of Ni-base alloys at high temperatures and (ii) inward oxides scale formation on low-Cr steels at moderate temperature.

4. Simulation of internal nitridation

Generally, internal corrosion phenomena including internal nitridation can be described by Wagner's theory of internal oxidation (Wagner, 1959) assuming a high thermodynamic stability of only one internally precipitating compound BO_v in an alloy AB and a substantially higher diffusion coefficient D_o of the corrosive species as compared to the one of the reacting alloying element D_B :

$$\xi^2 = \frac{D_o c_o^s}{\nu c_B^0} t \quad (17)$$

where ξ is the penetration depth of internal corrosion products, c_o^s the concentration of the corrosive species at the surface, and c_B^0 the initial concentration of the reacting alloying element.

A treatment of internal-corrosion problems that involve more than one precipitating species, compounds of moderate stability, high diffusivities of the metallic elements or time-dependent changes in the test conditions, e.g.

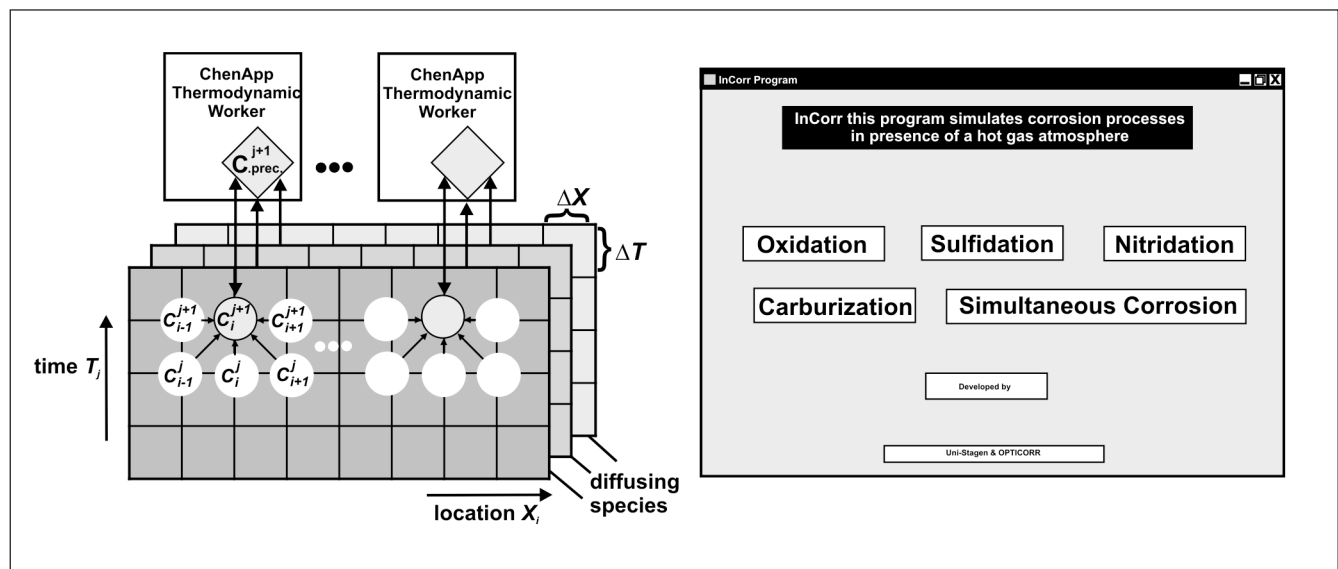


Figure 1 - (a) Schematic representation of the simulation procedure for internal corrosion combining the finite-difference algorithm with the thermodynamic program library ChemApp and (b) start window of the user-friendly interface of InCorr developed by using MATLAB.

temperature or interface concentrations, is not possible by applying Eq. (17). For simulation of such a system the combination of the finite-difference with a sophisticated thermodynamic program as described above is the most promising approach. Figure 2 gives an example for an InCorr calculation of the concentration profiles (Figure 2b) of the species involved in simultaneous internal precipitation of Ti and Al nitrides in a Ni-20Cr-2Al-2Ti alloy during high-temperature exposure in a nitrogen-based atmosphere (Krupp, 1998).

5. Simulation of inward oxide scale formation during oxidation of low-alloy steels

Figure 3a shows the typical oxide-scale structure on a low-Cr steel (X60, 1.43wt% Cr) after exposure at $T=550^{\circ}\text{C}$ to air. Generally, three layers can be identified, an outermost hematite (Fe_2O_3) layer, an outer magnetite ($\text{Fe}_3\text{O}__4$) layer and an inner magnetite layer, which gradually enriches in Cr forming FeCr_2O_4

double oxide. This is in agreement with the thermodynamic prediction using a specific data set developed for this kind of alloy (Trindade, 2006).

A closer look at the interface between inner scale and underlying metal reveals that inward oxide growth is governed by an intercrystalline oxidation mechanism. Supported by chemical analyses using energy-dispersive X-ray spectroscopy, it seems that the inward oxidation starts from the alloy grain boundaries initially forming

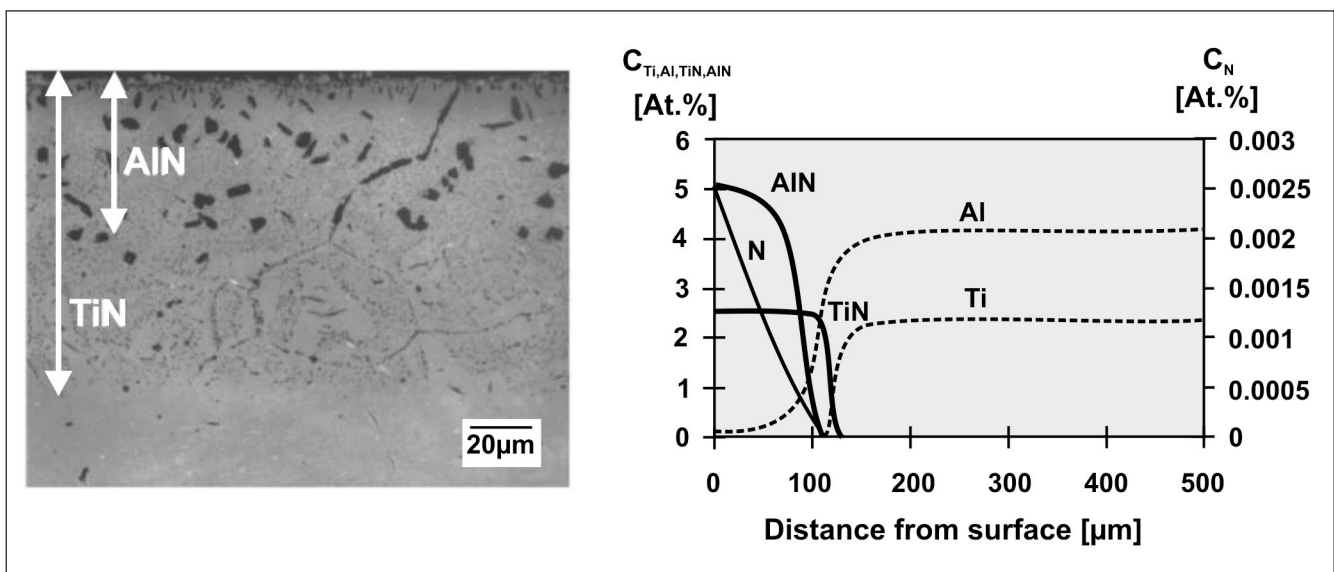


Figure 2 - Simultaneous internal nitridation by TiN and AlN in Ni-20Cr-2Al-2Ti (100h, 1000°C, nitrogen) (a) experimental result and (b) corresponding calculated concentration profiles (Krupp et al, 1999).

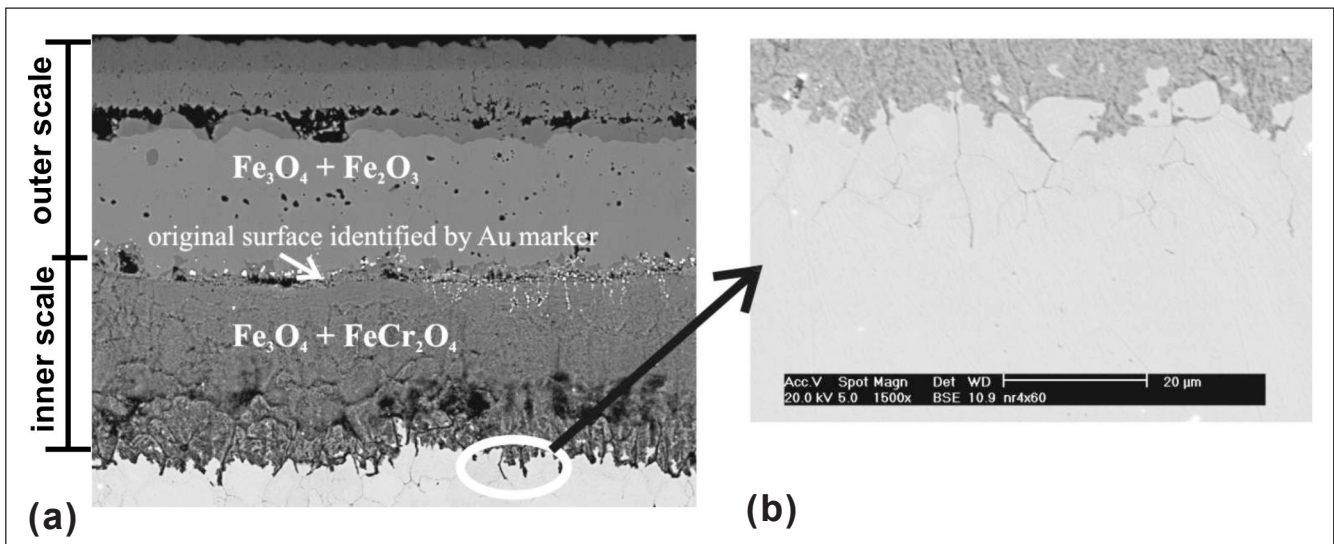


Figure 3 - (a) Oxide scale on a low alloy steel (grade X60) after exposure at 550°C to laboratory air for 72h and (b) detail, showing the grain boundary attack underneath the interface inner scale/metal.

Cr rich oxides, e.g., Cr_2O_3 and FeCr_2O_4 . From these oxidized grain boundaries oxidation proceeds into the grain interior forming FeCr_2O_4 and Fe_3O_4 .

To simulate inward oxidation of low-alloy steels, the oxygen concentration at the interface outer/inner scale is assumed to correspond to the oxygen partial pressure in equilibrium with Fe_3O_4 (2.0×10^{-16} bar at 550°C for steel containing 1.5wt% of Cr) and at the interface inner scale (GBs) to the underlying alloy to the oxygen partial pressure of Cr_2O_3 . Since useful diffusion data for O in porous Fe_3O_4 are not available, an effective diffusion coefficient has been derived based on the results of thermogravimetric measurements (Trindade, 2006). For the diffusion calculation a two-dimensional finite-difference approach with a moving boundary corresponding to the inward-growing inner scale/metal interface has been used (Figure 4). To account for the two-stage inward oxidation process, i.e. oxygen penetration along the grain-boundaries followed by bulk diffusion

into the grain interiors, the diffusion coefficient D is treated as location-dependent. For this purpose a diffusion matrix is used with individual D values for each grid in the finite difference mesh.

Due to the lack of data available for interface diffusivities, on the base of an estimate value for the grain boundary width (Heumann, 1992) of $d = 0.5\text{nm}$, the grain-boundary diffusion coefficient was assumed to be 100 times higher than the bulk diffusion coefficient, which has a value of $D_b = 5.39 \cdot 10^{-13}\text{m}^2/\text{s}$ for oxygen in iron at 550°C . No cross diffusion was taken into. Diffusion through the inner $\text{Fe}_3\text{O}_4/\text{FeCr}_2\text{O}_4$ scale, the mechanism of which is not fully understood since it strongly depends on the Cr concentration and is affected by the pronounced porosity, is treated in this study by an effective diffusion coefficient D_{eff} . The observed value of D_{eff} was estimated by means of the experimentally determined k_p value for the inner-scale growth kinetics in combination with Wagner's theory of oxidation.

$$k_p = \int_{p(\text{O}_2)_{\text{FeCr}_2\text{O}_4}}^{p(\text{O}_2)_{\text{Fe}_3\text{O}_4}} D_0 \, d \ln p(\text{O}_2) \quad (18)$$

where $p(\text{O}_2)_{\text{Fe}_3\text{O}_4}$ is the oxygen partial pressure at the outer/inner scale and $p(\text{O}_2)_{\text{FeCr}_2\text{O}_4}$ the estimated, respective pressure at the scale/substrate interface.

As an example of a diffusion simulation in Figure 5 an array of four grains was used. The results represent the concentration profiles of the species involved in the oxidation process of a Fe-1.43wt%Cr steel during 10h exposure at $T = 550^\circ\text{C}$ to air. The concentration profiles correspond to the experimental results for the inwards oxidation of this steel. The high thermodynamic stability of Cr_2O_3 enables its easy formation at the intergranular penetration front, even though the oxygen content is rather low. With the depletion of Cr in the vicinity of the grain boundaries, Fe will take part in the oxidation process, leading to the formation of the double oxide phase (FeCr_2O_4). As the oxygen potential increases, a part of FeCr_2O_4 will be further oxidized to form Fe_3O_4 .

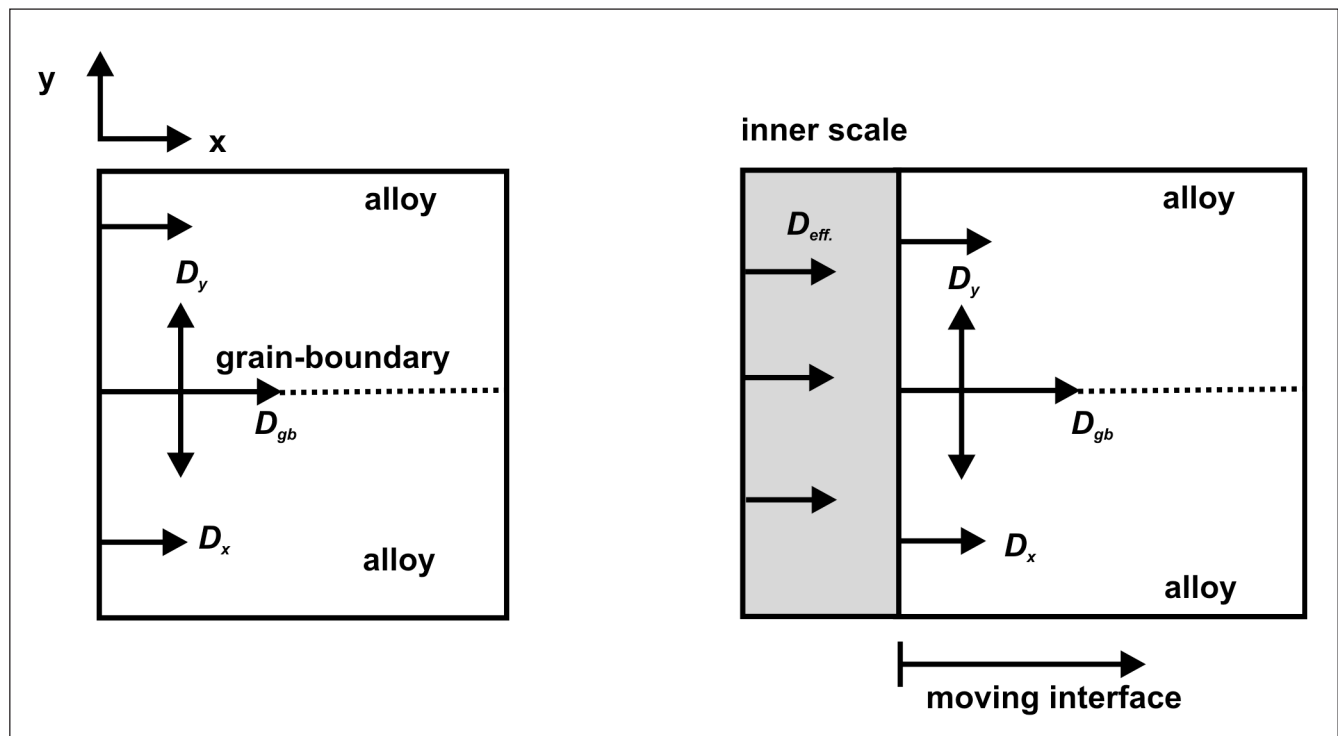


Figure 4 - Schematic representation of the diffusion mechanisms that are supposed to govern the inner oxide scale growth in low-alloy steels. (a) separation between grain-boundary (D_{gb}) and bulk diffusion (D_b) and (b) moving-boundary approach.

Applying the simulation to the same 1.43wt.%Cr steel with different grain sizes it revealed higher inner scale growth rates for fine-grained materials which is in excellent agreement with the experimental results (Trindade, 2006).

Figure 6 shows a comparison of the experimentally and the simulated measured inner-oxides as a function of the exposure time. The good agreement supports (a) the hypothesis that the proposed grain-boundary-oxidation mechanism determines the kinetics of inner scale growth, and (b) the applicability of the InCorr program to a great variety of diffusion- and thermochemically-controlled corrosion processes.

6. Conclusions

Diffusion-controlled corrosion processes like internal oxidation, nitridation, sulfidation, and carburization as well as superficial scale formation at high temperatures are determined by the diffusivities and the thermodynamic stabilities of the reacting species and the reaction products, respectively. To quantitatively describe such processes a finite-difference program InCorr has been developed in which a commercial powerful thermodynamic subprogram is implemented. This combination is capable to simulate a great variety of high-temperature corrosion processes. The successful application of the computer-simulation is shown by means of two examples, (i) internal nitridation of Ni-base alloys and (ii) inner-oxide-scale growth in low alloy steels. In both cases the comparison of experimental and simulation results yields an excellent agreement.

7. Acknowledgments

This research has been supported by the EU project OPTICORR, the Deutsche Forschungsgemeinschaft DFG, and the Brazilian Research Foundation (CAPES) through a fellowship to one of the authors (V.B. Trindade).

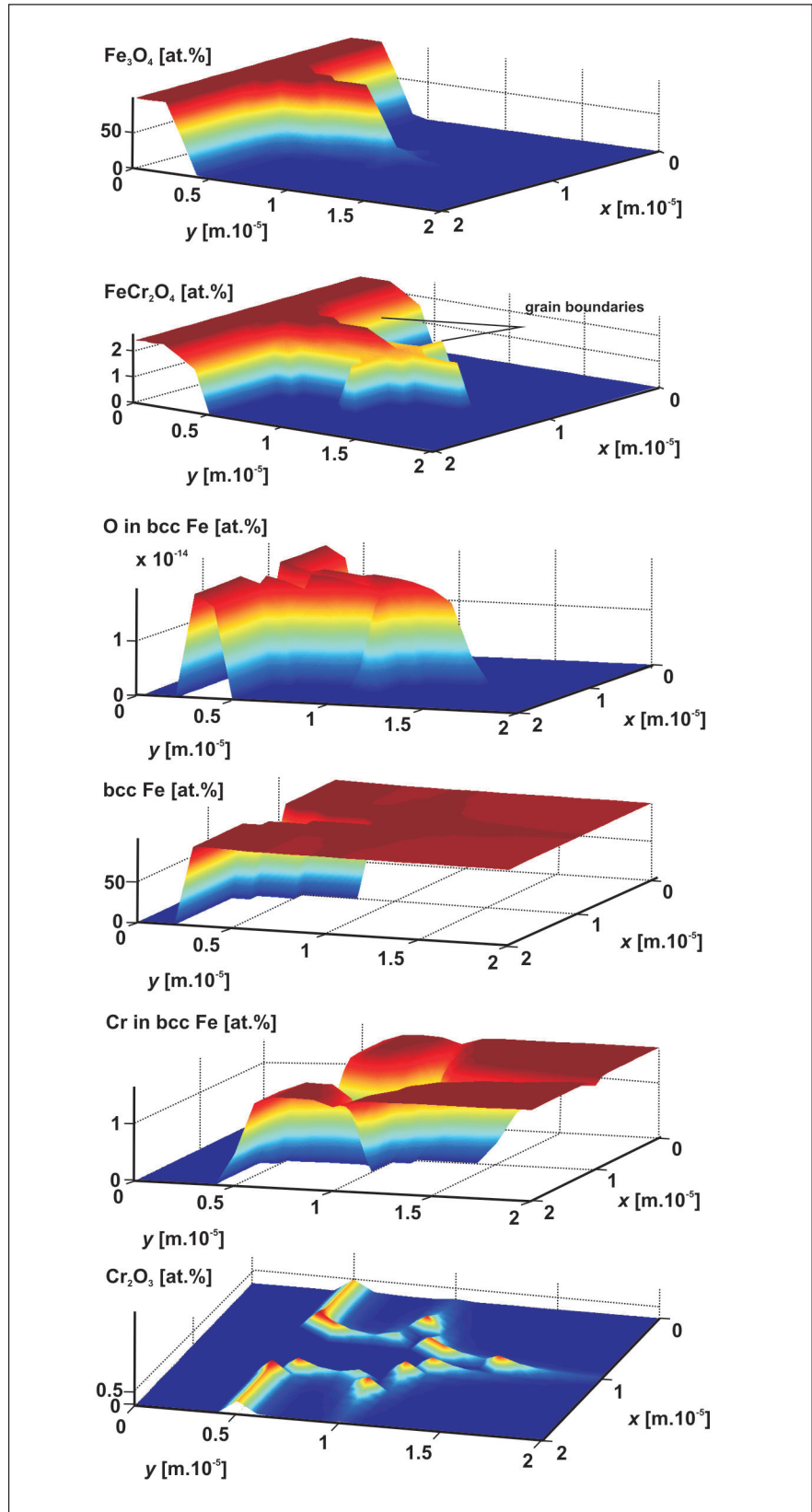


Figure 5 - Lateral concentration profiles of the species participating in the inner oxide scale formation process simulated by InCorr (Fe-1.43wt.%Cr, 550°C, air, $y=0$ corresponds to the original inner-scale/metal interface).

8. References

- CHRIST, H.J., CHRISTL, W. SOCKEL, H.G. Aufkohlung von Hochtemperaturwerkstoffen - Teil I: Modellmäßige mathematische Beschreibung des Vorganges der Eindiffusion mit gleichzeitiger Ausscheidung einer Verbindung des eindringenden Elementes. *Werkstoffe und Korrosion*, v. 37, p. 385-390, 1986.
- CRANK, J. *The mathematics of diffusion*. London: Oxford University Press, 1975.
- HEUMANN, T. *Diffusion in Metallen*, Berlin-Heidelberg: Springer-Verlag, 1992.
- KRUPP, U. *Innere Nitrierung von Nickelbasislegierungen*. Universität Siegen, 1998. (PhD Thesis).
- NESBITT, J.A. Numerical modeling of high-temperature corrosion Processes. *Oxidation of Metals*, v. 44, p. 309-338, 1995.
- SAVVA, G.C., WEATHEELY, G.C., KIRKALDY, J.S. Transition between Internal and External Nitridation of Ni-Ti Alloys. *Metallurgical and Materials Transaction A*, v. 27A, p.1611-1622, 1996.
- TRINDADE, V.B. Hochtemperaturoxidation chromlegierter Stähle und von nickelbasislegierungen: experimentelle untersuchung und computersimulation, Berichte aus der Materialwissenschaft, Schaker Verlag, Aachen, 2006.
- TRINDADE, V.B., KRUPP, U., CHRIST, H.J. InCorr-Software for Simulation of

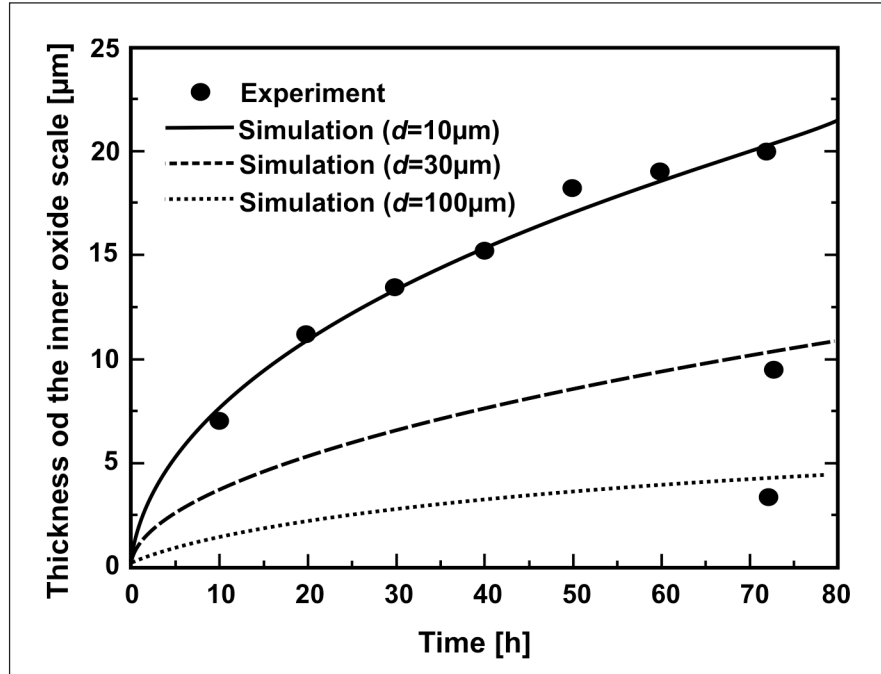


Figure 6 - Experimentally measured and simulated thickness of the inner oxide scale for different steel grain sizes (Fe-1.43wt.%Cr, $T=550^{\circ}\text{C}$, air).

- Internal/Inwards Corrosion at High Temperatures (chapter 3.1, p. 36-46) / Modeling of Internal Oxidation/Corrosion (chapter 4.2, p.102-115). In: BAXTER, D., HEIKINHEIMO, L. (Eds.). OPTICORR Guide Book. Finland: Espoo, 2005.
- VEDULA, K.M., A. W. FUNKENBUSCH, A.W., HECKEL, R.W. A mathematical model for internal oxidation. *Oxidation of Metals*, v. 16, p.385-395, 1981.
- WAGNER, C., Reaktionstypen bei der Oxydation von Legierungen. *Zeitschrift für Elektrochemie*, v. 63, p. 772-782, 1959.

Artigo recebido em 10/06/2008 e aprovado em 23/01/2009.

A REM tem novo endereço:
FUNDAÇÃO GORCEIX - REM
Rua Carlos Walter Marinho Campos, 57
Bairro: Vila Itacolomy
35400-000 - Ouro Preto - MG

www.rem.com.br